DOI: 10.1039/x0xx00000x

www.rsc.org/

Single dopant site imaging of covalently doped single-wall carbon nanotubes

Nicolai F. Hartmann,[‡a] Sibel E. Yalcin,[‡a] Lyudmila Adamska,[a,b] Erik H. Hároz,[a] Xuedan Ma,[a] Sergei Tretiak,[a,b] Han Htoon[a] and Stephen K. Doorn*[a]

Dual color images of doped SWCNTs

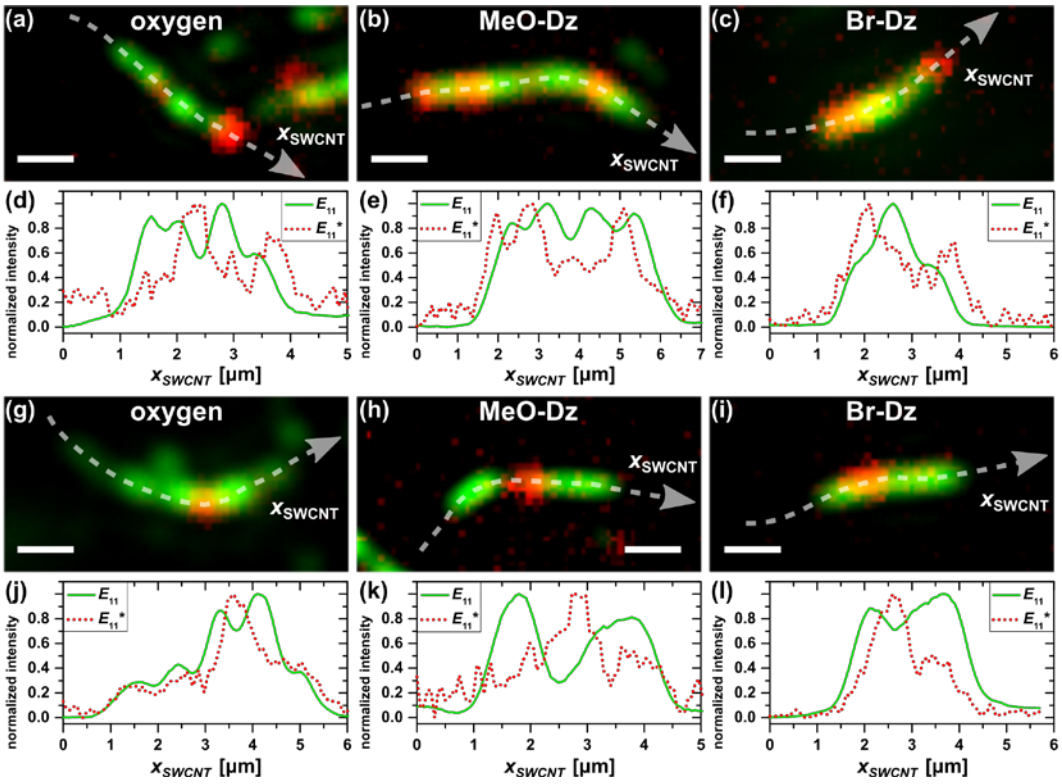

Fig. S1 Additional examples of solitary dopant imaging. Dual color images of oxygen (a), (g), MeO-Dz (b), (h) and Br-Dz (c), (i) doped individual SWCNTs. Single dopant site E11* emission (red channel) is visible along the pristine E11 emission (green channel) of the SWCNTs. The scale bar represents 1 µm in all images. Corresponding intensity cross sections along the SWCNT axes x_{SWCNT}, as indicated by the white dashed line in (a-c) and (g-i), are shown in the second and fourth row for the ozone doped (d), (j), MeO-Dz doped (e), (k) and Br-Dz doped (f), (i) SWCNTs.

[a] *Center for Integrated Nanotechnologies, Materials Physics and Applications Division, Los Alamos National Laboratory, Los Alamos, New Mexico 87545, United States.*
[b] *Theory Division, Los Alamos National Laboratory, Los Alamos, New Mexico 87545, United States.*
* skdoorn@lanl.gov
‡ Equal contribution

Position dependent spectra from single undoped and MeO-Dz doped SWCNTs

For obtaining position-dependent spectra the microscope setup, described in the main text, was equipped with a piezo driven scan stage (Nano-T series, Mad City Labs), controlled by a home-built LabView routine. Confocal excitation was reached by removing the lens focusing the excitation laser onto the back focal plane of the microscope objective. The detected signal was rerouted to a monochromator (Acton SP2300i) equipped with a 150 line/mm grating blazed at 1.2 µm. Spectra were then recorded on a linear InGaAs camera (Princeton Instruments LN/INGAAS-1024/500).

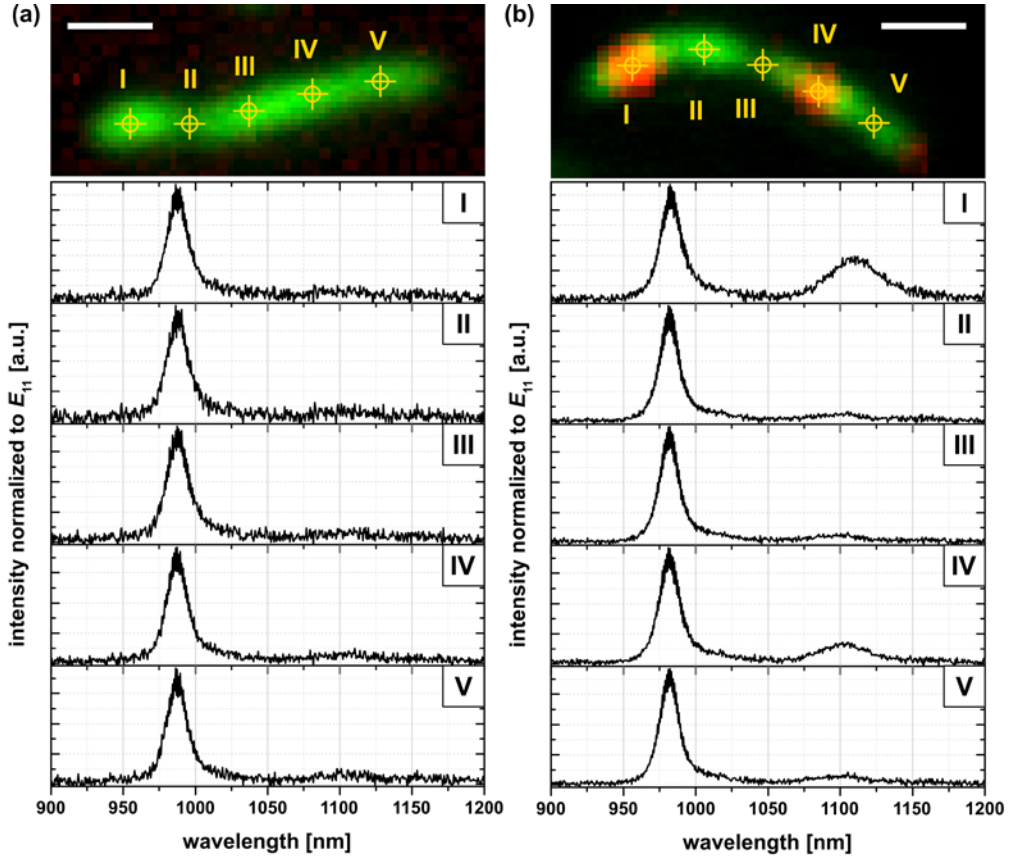

Fig. S2 Position dependent spectra of a single, undoped (a) and MeO-Dz doped (b) SWCNT. In the top row are shown dual color images of the undoped and MeO-Dz-doped SWCNTs. The scale bar represents 1 µm in both images. Positions at which spectra were taken are indicated by the yellow markers I – V. The corresponding spectra for each position and SWCNT are shown underneath each image. All intensities in the spectra are normalized to each E_{11} peak intensity. Note that the dopant emission peak only appears in spectra obtained from the doped tube and only from positions at which dopant emission is observed in the corresponding whole-tube images (spectra I and IV).

Diffusion lengths determined from nanotube end quenching.

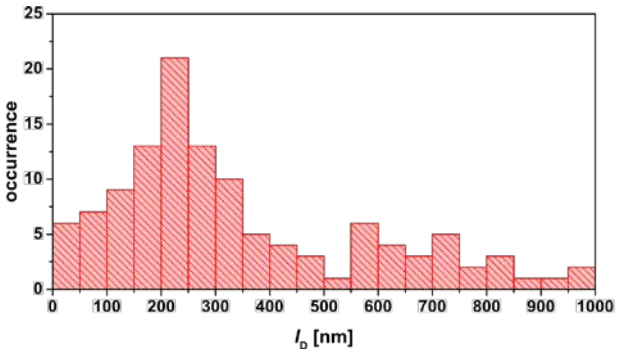

Fig. S3 Histogram of the diffusion lengths determined at both SWCNT ends for all doped nanotubes analysed in this manuscript .

The majority of fitted end diffusion lengths l_{left} and l_{right} according to equation (3) in the main text is situated around a mean value of 200±100 nm, equal to the diffusion lengths determined by the dopant site defects. However there is a non-negligible contribution of diffusion lengths at the SWCNT ends larger than 500 nm (as shown in Fig. S3). These can be understood in terms of dopant sites occurring close to the SWCNT ends that do not emit during the observed time period. In this case the end diffusion length is overestimated by the fitting.

Density Functional Theory Calculations.

Atomic structure of the doped CNTs

Figure S4 displays the atomistic structures of (6,5) SWCNTs in the vicinity of the different dopant sites investigated computationally. The top row shows the three most stable geometries of ozonated SWCNTs. The first structure ((a) O-ether-d) is the most energetically stable configuration,[1] thus it was further employed for our simulations of the electrostatic potential in a long nanotube. The bottom row of Fig. S4 portrays the two diazonium species considered in this work.

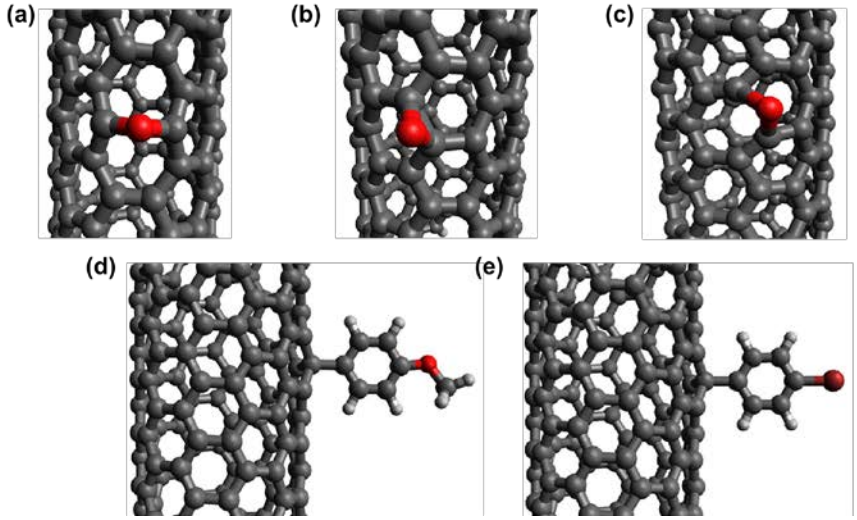

Fig. S4 Atomistic structures of doped (6,5) nanotubes. The top row depicts three considered defect geometries in ozonated CNTs, ether-d (a), epoxide-l (b) and ether-l (c). In the bottom row the two diazonium doped species MeO-Dz (d) and Br-Dz (e) are shown. Grey, red, brown and white balls correspond to carbon, oxygen, bromine, and hydrogen atoms, respectively.

Structural stability of dopants

The formation energies of oxygen dopants in (6,5) SWCNTs were computed in references [1] and [2]. It was shown that the ether-d oxygen configuration (O binds to two C atoms while breaking a C-C bond aligned perpendicular to the SWCNT axis) is the most stable structure. In this work, three Oxygen dopant geometries were considered, see top row of Fig. S4. The total energies of epoxide-l and ether-l structures are 1.15 eV and 1.48 eV higher than that of ether-d, respectively. The relative total energies of O-doped structures and the diffusion activation energies E_a are compiled in Fig. S5.

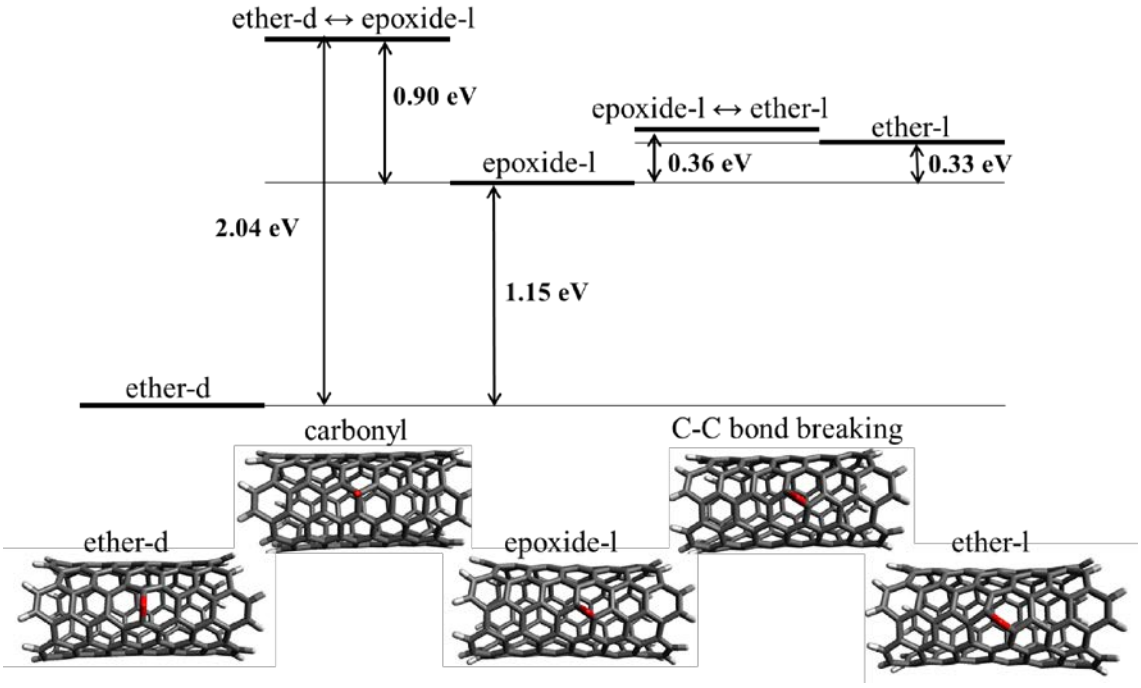

Fig. S5 Schematic representation of energy scales for the binding energy and diffusion barriers of Oxygen adatoms in ozonated SWCNTs. The atomistic structures of defect geometries and transition state configurations are shown under each considered case.

The lifetime τ of the particular Oxygen doping configuration may be estimated from the Arrhenius law $k = k_0 e^{-E_a/k_B T}$ where the lifetime is inversely proportional to the rate $k = 1/\tau$. The rate constant k_0 for carbon materials typically varies from 10^{10} to 10^{13}. This results in a lifetime of the ether-d configuration at room temperature $k_B T = 0.025$ meV of $2.8\times(10^{22}\text{-}10^{25})$ seconds, thus ether-d will not undergo migration. Epoxide-l, in contrast, has a 0.9 eV barrier to convert into ether-d, which corresponds to a configuration lifetime of about $4.3\times(10^{2}\text{-}10^{5})$ seconds, e.g. minutes to days. Epoxide-l can, in principle, also convert into a higher energy configuration ether-l, but given the short lifetime of both structures, it is highly unlikely that epoxide-l↔ether-l fluctuations will contribute to blinking because the timescales do not match.

In the case of aryl-type dopants, the binding energy of an aryl ring is about 1.5 eV. The transition state geometry, corresponding to hopping of the aryl ring from one carbon atom in the nanotube to its nearest-neighbor carbon atom, is the breaking of C-C bond between the SWCNT and the aryl ring. Thus, we conclude that diffusion of the aryl ring is equivalent to desorption. Diazonium species are very stable dopants and they do not migrate.

Electrostatic potential maps

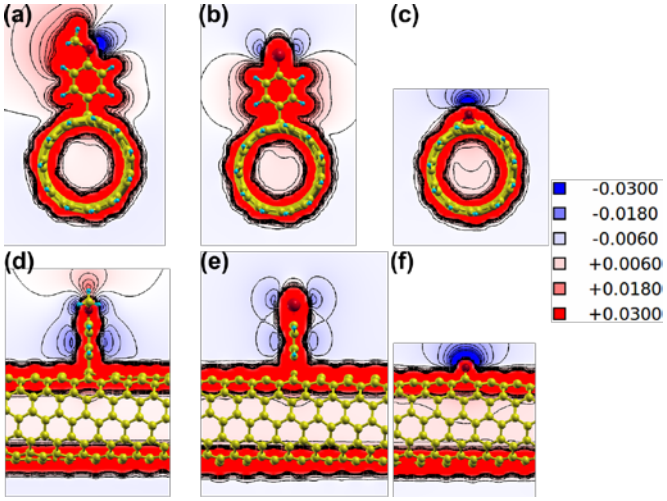

Fig. S6 Electrostatic potential maps of a MeO-Dz doped (a), Br-Dz doped (b) and oxygen doped (c) SWCNT with the viewing direction along the SWCNT axis. In the second row the corresponding side views are shown for the MeO-Dz doped (d), Br-Dz doped (e) and oxygen doped (f) SWCNT. Inset provides the different values of the isosurfaces (arbitrary units)

As discussed in the main text, the top row of contour maps in Fig. S6 (a-c) best show dopant perturbation of the electrostatic potentials in the radial direction. The axial extent of the perturbation is shown in Fig. S6 (d-f) and is found to be ≈ 1 nm in extent for oxygen, while perturbation by other dopants is more limited in the axial direction.

References

1 X. Ma, L. Adamska, H. Yamaguchi, S. E. Yalcin, S. Tretiak, S. K. Doorn and H. Htoon, *ACS Nano*, 2014, 8, 10782-10789.
2 M. Ohfuchi, *J. Phys. Chem. C*, 2015, **119**, 13200.